J. Membrane Biol. 95, 73–89 (1987)

The Journal of
Membrane Biology
© Springer-Verlag New York Inc. 1987

How do Protons Cross the Membrane-Solution Interface? Kinetic Studies on Bilayer Membranes Exposed to the Protonophore S-13 (5-chloro-3-tert-butyl-2′-chloro-4′nitrosalicylanilide)

John Kasianowicz†, Roland Benz‡, and Stuart McLaughlin†

†Department of Physiology and Biophysics, State University of New York, Stony Brook, New York 11794, and ‡Lehrstuhl für Biotechnologie, Universität Würzburg, D-8700 Würzburg, Federal Republic of Germany

Summary. A simple carrier model describes adequately the transport of protons across lipid bilayer membranes by the weak acid S-13. We determined the adsorption coefficients of the anionic, A^-, and neutral, HA, forms of the weak acid and the rate constants for the movement of A^- and HA across the membrane by equilibrium dialysis, electrophoretic mobility, membrane potential, membrane conductance, and spectrophotometric measurements. These measurements agree with the results of voltage clamp and charge pulse kinetic experiments. We considered three mechanisms by which protons can cross the membrane-solution interface. An anion adsorbed to the interface can be protonated by (i) a H^+ ion in the aqueous phase (protolysis), (ii) a buffer molecule in the aqueous phase or (iii) water molecules (hydrolysis). We demonstrated that the first reaction cannot provide the required flux of protons: the rate at which H^+ must combine with the adsorbed anions is greater than the rate at which diffusion-limited reactions occur in the bulk aqueous phase. We also ruled out the possibility that the buffer is the main source of protons: the rate at which buffers must combine with the adsorbed anions is greater than the diffusion-limited rate when we reduced the concentration of polyanionic buffer adjacent to the membrane-solution interface by using membranes with a negative surface charge. A simple analysis demonstrates that a hydrolysis reaction can account for the kinetic data. Experiments at acid pH demonstrate that the transfer of H^+ from the membrane to the aqueous phase is limited by the rate at which OH^- combines with adsorbed HA and that the diffusion coefficient of OH^- in the water adjacent to the bilayer has a value characteristic of bulk water. Our experimental results demonstrate that protons are capable of moving rapidly across the membrane-solution interface, which argues against some mechanisms of local chemiosmosis.

Key Words local chemiosmosis · protonophores · protons · bilayers · uncouplers · S-13

Introduction

McLaughlin and Dilger [37] and Terada [50] have reviewed the transport of protons across membranes by weak acids; we refer the interested reader to these papers for a detailed discussion of the older literature. The simplest mechanism by which a weak acid, such as FCCP (carbonyl cyanide *p*-trifluoromethoxyphenylhydrazone [5]), CCCP (carbonyl cyanide *m*-chlorophenylhydrazone [29, 43]) or S-13, could transport protons across a bilayer membrane is illustrated in Fig. 1*a*. These weak acids can function as proton carriers, or protonophores, because both the anionic, A^-, and neutral, HA, forms of the weak acid adsorb strongly to the membrane-solution interface by means of hydrophobic interactions and because both A^- and HA partition into and permeate the interior of the membrane [5, 29, 37]. There are three reasons why the anionic form of the protonophores is soluble in the low dielectric interior of the lipid bilayer: the π electrons of the weak acid delocalize the charge and reduce the Born energy [15, 42, 44] required to move the anion from water into the membrane, the hydrophobic groups favor partitioning into the membrane, and the dipole potential of the phospholipid bilayer (about 200–300 mV positive inside [16, 17, 27]) favors the partitioning of the anion into the bilayer. This latter factor presumably accounts for the observation that all common protonophores are weak acids rather than weak bases.

We are interested in the molecular mechanism by which weak acids transport protons across membranes for two reasons. First, there is still some controversy about the mechanism of energy transduction in mitochondria, chloroplasts and bacteria. The chemiosmotic hypothesis postulates that oxidation is coupled to phosphorylation in mitochondria by means of a difference in the electrochemical potential of protons between the two bulk aqueous phases, $\Delta\tilde{\mu}_{H^+}$ [39]. It follows that all protonophores should uncouple oxidation from phosphorylation by reducing the magnitude of $\Delta\tilde{\mu}_{H^+}$. The chemical hypothesis postulates that protons are not involved directly in energy coupling and that weak acids act as uncouplers by interacting specifically with components of the electron transport chain [22, 30, 31].

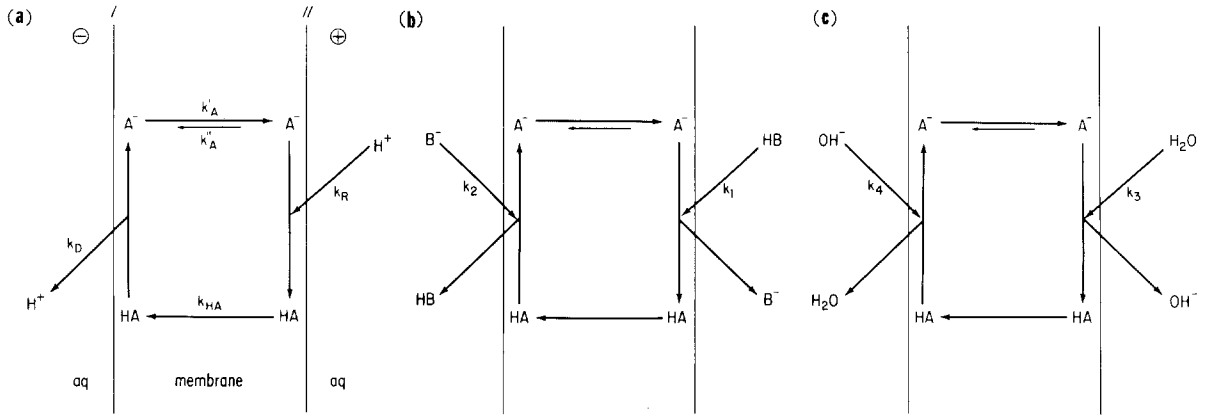

Fig. 1. The mechanism by which S-13 transports protons across lipid bilayer membranes. The circled positive and negative signs indicate there is a potential difference across the membrane. The rate constants k'_A and k''_A refer to the voltage-dependent translocation of the anion A^- from the ′ to the ″ and from the ″ to the ′ interfaces, respectively. The rate constant k_{HA} refers to the movement of HA between the two interfaces. We consider three possible mechanisms for delivery of protons to the adsorbed anion. (*a*) A proton in the aqueous phase, *aq*, combines with an adsorbed anion. The rate constants k_R and k_D refer to the heterogeneous recombination and dissociation of an aqueous proton with an anion adsorbed to the membrane. (*b*) A buffer molecule in the aqueous phase collides with and transfers a proton to an adsorbed anion. (*c*) Hydrolysis of water molecules deliver protons to the adsorbed anions

However, Terada and Van Dam [51] have shown that less than 0.2 molecule of the potent uncoupler SF6847 (3,5-di(tert-butyl)-4-hydroxybenzylidene-malononitrile) per respiratory chain is sufficient to uncouple mitochondria. Although the chemical hypothesis is moribund if not dead, the role of protons in energy coupling is still controversial. Many investigators argue that a localized gradient of protons could couple oxidation to phosphorylation [54, 55]. The elegant experiments of Hackenbrock and his coworkers [18] demonstrate that the components of the electron transport chain diffuse sufficiently rapidly in the mitochondrial membrane that protons could, in principle, be transferred directly by collision between these macromolecules without equilibrating with the bulk aqueous phase. This version of the local chemiosmotic hypothesis, however, cannot easily explain why weak acid protonophores act as uncouplers.

Second, we are interested in the mechanisms by which protons cross membrane-solution interfaces. A simple model (Fig. 1*a*) can account for most of the kinetic data obtained with FCCP and CCCP. We noted [5], however, that the apparent rate constant for the recombination of a proton with an adsorbed anion of FCCP (k_R in Fig. 1*a*) is slightly larger than the value characteristics of a diffusion-limited reaction in a bulk aqueous phase, 10^{10}–10^{11} M^{-1} sec^{-1} [4, 12]. The voltage clamp and charge pulse data we obtained with the protonophore S-13 (*see below*) require a rate constant $k_R > 10^{13}$ M^{-1} sec^{-1} to be consistent with the model illustrated in Fig. 1*a*. This rate constant is two orders of magnitude faster than the value for a diffusion-limited reaction in a bulk aqueous phase.

One interesting possibility is that the mechanism illustrated in Fig. 1*a* is valid and that k_R is large because protons can diffuse very rapidly in the "reaction layer," of thickness 1–10 nm, adjacent to a bilayer membrane[1]. However, Nachliel and Gutman [40] found that protons do not diffuse anomalously rapidly in the water adjacent to membranes[2].

[1] When we apply a voltage across the membrane and protons move between the two bulk aqueous phases, the reaction between a proton and the anionic form of the buffer is in equilibrium throughout most of the aqueous unstirred layer (*see* reference [41] and footnote 3). However, if the mechanism illustrated in Fig. 1*a* is operative, equilibrium cannot be maintained in the "reaction layer," the region immediately adjacent to the membrane [33]. The exact treatment of this problem, which involves simultaneous diffusion and chemical reaction, is discussed on pp. 87–95 of Delahay [7]. The thickness of the reaction layer is about 1 nm when the concentration of buffer is 0.1 M and about 10 nm when the concentration of buffer is 0.001 M.

[2] We do not accept the recent claim of Tocanne and his coworkers [46, 49] that diffusion of protons adjacent to phospholipid monolayers is "20 times faster than in the bulk water phase." We suggest that stirring produces a convective flow of lipids in their monolayer, which drags along the aqueous unstirred layer[3] that contains protons at high concentration. There are two reasons for believing that their results are due to a convection artifact rather than a fast diffusion of protons. First, they measured a lipid diffusion coefficient of 7×10^{-4} cm^2 sec^{-1}, which is four orders of magnitude higher than the accepted values for the diffusion coefficient of a lipid in a bilayer or monolayer. Second, even if protons do diffuse rapidly in a narrow (<10 nm) region adjacent to the bilayer, which has some properties different from those of bulk water [28, 45], their measurement would not have detected this rapid movement. Our experimental results demonstrate that protons adjacent to the bilayer must exchange very rapidly with protons in the bulk aqueous

Another possibility is that the acidic form of the buffer, which is present in relatively high concentrations in the aqueous phase (*see* Fig. 1*b*), donates the proton to the adsorbed anion [5]. The protonophore data in the literature are consistent with this mechanism if the rate constant for the transfer of a proton from the aqueous buffer, HB, to the anion adsorbed to the membrane, A^-, is $k_1 > 10^8$ M^{-1} sec^{-1}. This postulate is reasonable because all "normal" weak acids transfer protons with rate constants $>10^8$ M^{-1} sec^{-1} in the favorable direction [4]. Thus the mechanisms in Fig. 1*a* and *b* should act in parallel. Are they sufficient to account for all the experimental observations?

It would appear to be simple to answer this question experimentally. If the concentration of buffer in the aqueous phase is reduced, it would not deliver protons sufficiently rapidly to the A^- form of S-13. This would displace the protonation reaction at the interface from equilibrium and cause marked changes in the kinetic voltage clamp and charge pulse data. Unfortunately, our experiments require >1 mM buffer in the aqueous phase to facilitate the diffusion of protons through the Nernstian aqueous unstirred layers[3] by the "buffer shuttle mechanism" [19]; if [HB] < 1 mM, the proton concentration increases on one side of the membrane and decreases on the other side when a voltage is applied. This diffusion polarization [33] confounds any simple analysis of the data.

We attempted to circumvent this problem by incorporating negatively charged lipids into the membrane and using a polyanionic buffer. The relatively high concentration of buffer in the aqueous unstirred layer (1 mM) prevents any significant diffusion polarization of protons; the negative surface potential lowers markedly (<1 μM) the concentration of buffer in the aqueous electrostatic diffuse double layer (thickness <1 nm under our experimental conditions [36]) immediately adjacent to the membrane. Under these conditions, the buffer cannot deliver protons at a rate sufficient to maintain the interfacial reactions at equilibrium. If Fig. 1*b* represents the dominant mechanism for proton transfer across the membrane-solution interface, we should have observed marked changes in the voltage clamp and charge pulse kinetic data. We did not observe any changes. The protonation reactions illustrated in Fig. 1*a* and *b* remained at equilibrium.

Finally, we consider the possibility that the proton is delivered to the adsorbed anion directly from water molecules (*see* Fig. 1*c*). A simple calculation (*see* Appendix II) indicates that hydrolysis can account for the large flux of protons across the interface of a bilayer membrane exposed to the protonophore S-13. It also predicts that the release of protons from the left-hand interface in Fig. 1*c* should be limited by the $[OH^-]$ at acid pH. The results of our kinetic voltage-clamp and charge-pulse experiments agree with this prediction. We can describe adequately these kinetic results if we assume the diffusion coefficient of OH^- in the water immediately adjacent to the membrane has the same value as in bulk water. Eigen [11] discusses in detail the protolysis, buffer transfer, and hydrolysis reactions considered here.

In summary, a proton moves through most (99.99%) of the aqueous unstirred layer by means of a buffer shuttle mechanism [19]. When it reaches the reaction layer, the three mechanisms illustrated in Fig. 1; (*a*) proton diffusion and reaction, (*b*) buffer diffusion and proton transfer, and (*c*) hydrolysis; act in parallel to transfer protons to the membrane.

Theory

The simple carrier mechanism illustrated in Fig. 1 can account for the ability of the weak acid S-13 to act as proton ionophore. We described the kinetic model in detail for FCCP [5]. We outline here the main assumptions of the model, listing only the equations we use to calculate the transport parameters from the experimental results.

A major assumption of our model (Fig. 1) is that the anion, A^-, is the only charged species that moves across the interior of the membrane; it moves with voltage-dependent translocation rate constants k'_A and k''_A (Fig. 1*a*). In Fig. 1*a*, the anion adsorbed to the interface recombines with protons from the aqueous phase with a heterogeneous reaction rate constant k_R: the HA molecules adsorbed to the interface dissociate with a rate constant k_D. The equilibrium association constant is $K = k_R/k_D$ and $\log(K)$ is the surface pK. In Fig. 1*b* and *c*, buffer and water molecules donate protons to the ad-

phase. The diffusion coefficient in the adjacent semi-infinite aqueous phase is $\sim 10^{-4}$ cm^2 sec^{-1}; if the protons diffuse a distance $\geqslant 10$ nm the measured diffusion coefficient must approach this value. Their measurements were made over large distances (centimeters) and long times (hundreds of seconds).

[3] Irrespective of how fast one mixes the bulk of a solution, the fluid velocity adjacent to the surface will be low and there will be a layer that remains essentially unmixed or stagnant. The movement of solutes through these "unstirred layers" is usually treated in the Nernstian manner, an approximation discussed briefly by both Helfferich [24] and McLaughlin and Eisenberg [38], and in more detail by Vetter [53]. One assumes solutes move only by diffusion through the unstirred layer and the solution outside this layer is perfectly mixed. The thickness of these layers is about 100 μm for a planar surface in contact with a well-stirred solution [6, 14, 23, 26]. The flux of protons through these unstirred layers is greatly enhanced by buffers; the buffer shuttle mechanism is discussed by Gutknecht and Tosteson [19].

sorbed anion. The diffusion of the neutral form of S-13, HA, across the membrane is assumed to be independent of voltage; the translocation rate constant is k_{HA}. It is easy to demonstrate [5] that the total number of S-13 molecules adsorbed to the membrane, N_o, does not change significantly during a kinetic experiment:

$$N_o = 2N_A + 2N_{HA} \tag{1}$$

where N_A and N_{HA} are the surface concentrations of A^- and HA adsorbed to one interface. The equilibrium adsorption coefficients are defined by:

$$\beta_A = N_A^o/[A^-] \tag{2}$$

$$\beta_{HA} = N_{HA}^o/[HA] \tag{3}$$

where $[A^-]$ and [HA] denote the bulk aqueous concentrations of the anionic and acidic forms of S-13, N_A^o and N_{HA}^o denote the equilibrium surface concentrations of A^- and HA.

Our kinetic experiments with FCCP [5] and CCCP [29] demonstrated that the interfacial protonation reactions illustrated in Fig. 1 remain at equilibrium, even when a large voltage (200 mV) is applied to the membrane. We assume that for S-13 the interfacial reactions also remain at equilibrium for pH > 7.3, an assumption consistent with our kinetic voltage clamp and charge pulse results. In this case Eq. (4) is approximately valid throughout the relaxation process:

$$N'_{HA}/N'_A = N''_{HA}/N''_A = K[H^+]. \tag{4}$$

This assumption greatly simplifies the kinetic equations that describe the experimental data [5]. In Appendices I and II we calculate the values of k_R and k_3 (*see* Fig. 1) required to account for the experimental data and argue that the protons cross the membrane-solution interface mainly by the mechanism illustrated in Fig. 1*c*.

Under voltage-clamp conditions the system is at equilibrium for times $t < 0$; at $t = 0$ a voltage V is applied across the membrane. The current density, $I(t)$, depends on time in the following manner if the capacitance spike is ignored:

$$I(t) = F(k''_A N''_A - k'_A N'_A) = I(\infty)[1 + \alpha\exp(-\lambda t)] \tag{5}$$

where F is the Faraday and $I(\infty)$ is the steady-state current density. The relaxation amplitude, α, is related to the rate constants and surface pK by

$$\alpha = (k'_A + k''_A)/2K[H^+]k_{HA}. \tag{6}$$

The time constant, $\tau \equiv 1/\lambda$ is related to the rate constants and surface pK by

$$\lambda = (k'_A + k''_A + 2k_{HA}K[H^+])/(1 + K[H^+]). \tag{7}$$

Note that both the amplitude and time constant of the relaxations are independent of the [S-13].

The shape of the potential energy barrier that A^- encounters within the membrane influences the voltage dependence of k'_A and k''_A. This barrier is due mainly to "image" forces and can be described by a trapezoid [8, 21, 25]. If the minor base of the trapezoid spans a fraction b of the membrane the voltage dependence of k'_A and k''_A is given approximately[4] by

$$k'_A = k_A(bu/2)\exp(u/2)/\sinh(bu/2) \tag{8}$$

$$k''_A = k_A(bu/2)\exp(-u/2)/\sinh(bu/2). \tag{9}$$

It is apparent from Eqs. (5), (8) and (9) that the instantaneous current, $I(0)$, is proportional to $\sinh(u/2)$ when $b \to 0$ (triangular barrier), whereas $I(0)$ is proportional to u when $b \to 1$ (square barrier). In the limit of small voltages, $u \ll 1$, k'_A and k''_A do not depend on the shape of the barrier:

$$k'_A = k_A(1 + u/2) \tag{10}$$

$$k''_A = k_A(1 - u/2). \tag{11}$$

The instantaneous conductance measured in the limit of a low applied voltage, $G(0, 0)$, is given by

$$G(0, 0) = F^2\beta_A[A^-]k_A/RT. \tag{12}$$

Under charge pulse conditions, we assume the membrane capacitance C_m is charged to a voltage $V^o \ll 25$ mV at $t = 0$. We can describe the subsequent decay in voltage by the sum of 2 exponential relaxations [5]:

$$V(t) = V^o[a_1\exp(-\lambda_1 t) + a_2\exp(-\lambda_2 t)] \tag{13}$$

where the time constants, $\tau_1 = 1/\lambda_1$ and $\tau_2 = 1/\lambda_2$, and the relative amplitudes of the relaxations, a_1 and a_2, are given by Eqs. (14)–(16):

$$\lambda^2 - \lambda(Bk_A N_o + 4k_A + 4k_{HA}K[H^+])/2(1 + K[H^+]) + (BK[H^+]k_A k_{HA}N_o)/(1 + K[H^+])^2 = 0 \tag{14}$$

$$a_1 + a_2 = 1 \tag{15}$$

$$a_1\lambda_1 + a_2\lambda_2 = Bk_A N_o/2(1 + K[H^+]) \tag{16}$$

where $B = F^2/RTC_m$.

The rate constants k_A and k_{HA} cannot be obtained directly from a single charge pulse measure-

[4] A more exact analysis of the equations in Hladky [25] yields conductance-voltage curves that differ by less than 20% from those predicted by the combination of Eqs. (5), (8) and (9) for voltages less than 200 mV.

ment made at a given pH. Therefore, we define the quantities K_A and K_{HA}, which can be calculated from the analysis of a single charge pulse measurement:

$$K_{HA} = k_{HA}K[H^+]/(1 + K[H^+]) \quad (17)$$

$$K_A = k_A/(1 + K[H^+]). \quad (18)$$

Materials and Methods

The unilamellar vesicles used for the equilibrium dialysis experiments were formed from egg phosphatidylcholine (egg PC; Avanti Polar Lipids, Birmingham, AL). The lipid was sonicated in a 0.1 M NaCl (Fisher Scientific, Fairlawn, NJ) solution buffered to pH 10 with 0.05 M CAPS (3-cyclohexylamino-1, 1-propanesulfonic acid; P-L Biochemicals, Milwaukee, WI), then centrifuged [3]. The dialysis experiments were performed at 21°C in Teflon chambers. We equilibrated the dialysis membrane with the appropriate concentration of S-13 before the experiment because of significant (30%) loss of protonophore in control experiments. The lipid concentration in the *cis* side of the chamber was measured by phosphate analysis [35]. The S-13 concentration in both the *cis* and *trans* compartments was measured spectrophotometrically to ensure that no significant adsorption of S-13 to the chamber occurred. S-13 (Fig. 2) was a gift from Drs. D. Wilson and E. Bamberg, who originally obtained the compound from Monsanto Chemical Co. (St. Louis, MO).

We prepared the multilamellar vesicles for the microelectrophoresis experiments from egg PC [2] and measured the electrophoretic mobilities at 25°C in a Rank Bros. (Bottisham, Cambridge, U.K.) Mark I machine. The 0.1, 0.01 and 0.001 M NaCl solutions were buffered to pH 8.5 with 1, 1 and 0.1 mM TRIS, respectively. The solutions also contained 5 μM EDTA to remove trace concentrations of multivalent cations.

Planar black lipid membranes for the membrane potential, voltage clamp and charge pulse measurements were formed from a 1–2% (wt/vol) solution of lipid in either 1-*n*-chlorodecane (Aldrich Chemical, Milwaukee WI) or *n*-decane (Supelco, Belefonte, PA). The chlorodecane was passed through an aluminum oxide column to remove impurities (Baker, Phillipsburg, NJ). Bacterial phosphatidylethanolamine (PE), bacterial phosphatidylglycerol (PG) and diphytanoyl PC were obtained from Avanti Polar Lipids (Birmingham, AL). The water used to prepare the aqueous solutions was deionized with a Millipore Super Q system (Millipore, Bedford, MA), then distilled twice in a quartz still. The aqueous solutions contained either 0.1 or 1 M NaCl and buffer: HEPES (N-2-hydroxyethylpiperazine-N'-2-ethanesulfonic acid), Bicine (N,N-bis(2-hydroxyethyl)glycine), Tricine (N-tris(hydroxymethyl)methylglycine), Tris (tris(hydroxymethyl)aminomethane), EPPS (N-2-hydroxyethylpiperazine-N'-3-propanesulfonic acid), all obtained from P-L Biochemicals (Milwaukee, WI), as well as phosphate, triphosphate, and tetraphosphate, from Sigma Chemical Co. (St. Louis, MO).

The experiments with planar bilayers were performed at room temperature (20–22°C) in Teflon cells. The membranes were formed on a hole of 1–2 mm diameter in the thin Teflon wall separating two aqueous compartments. Small aliquots of S-13 dissolved in ethanol were added to the aqueous phases. The concentration of ethanol in the Teflon cell never exceeded 0.5% and had no significant effect on the experimental results. We described the equipment and experimental protocol used for kinetic voltage clamp and charge pulse measurements previously [5]. The initial conductance of diphytanoyl PC/chlorodecane membranes formed from different batches of lipid varied by a factor of two. The time resolution of the charge pulse measurements was about 200 nsec in 1 M NaCl and about 1 μsec in 0.1 M NaCl. Ag/AgCl electrodes with liquid junctions were used with a Keithley Instruments (Cleveland, OH) 602 electrometer to measure the membrane potential when the membrane separated two solutions of different pH. In these experiments the aqueous phases contained 0.1 μM S-13, 0.1 M NaCl, 0.1 M $NaHCO_3$, 0.1 M Na_2HPO_4, and 0.05 M $Na_2B_4O_7$ and the membranes were formed from a solution of diphytanoyl PC in decane. The steady-state conductance measurements used to determine the aqueous pK of S-13 were also made with a Keithley 602 electrometer.

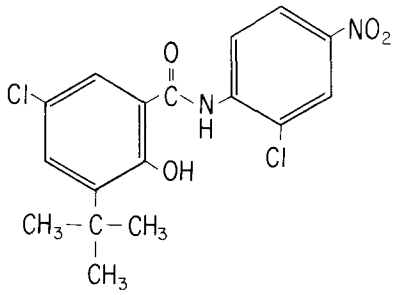

Fig. 2. The chemical structure of S-13. Note the π electrons delocalize the charge on the A^- form of S-13

Results

Independent Measurements

Whenever possible we determined the parameters necessary to characterize the kinetic model illustrated in Fig. 1 by making direct measurements.

Determination of β_A

We determined the adsorption coefficient of the anionic form of S-13 onto phosphatidylcholine (PC) membranes in three different ways. First, we made equilibrium dialysis measurements with sonicated egg PC vesicles. These measurements were conducted at pH 10, where essentially all the S-13 is in the anionic form. We obtained a value of $\beta_A = (3 \pm 0.3)\ 10^{-2}$ cm.

Second, we determined the adsorption coefficient of the A^- form of S-13 onto multilamellar egg PC vesicles from microelectrophoresis measurements. Figure 3 illustrates the effect of S-13 on the zeta potentials of PC vesicles. The curves are the predictions of the Stern equation, a combination of the Gouy equation, the Boltzmann relation and a linear (Henry's law) adsorption isotherm [29]. We obtain a good fit to the data at all [NaCl] if the adsorption coefficient, β_A, the only adjustable parameter, is taken to be 3×10^{-2} cm. The strong adsorption of S-13 to bilayer membranes is charac-

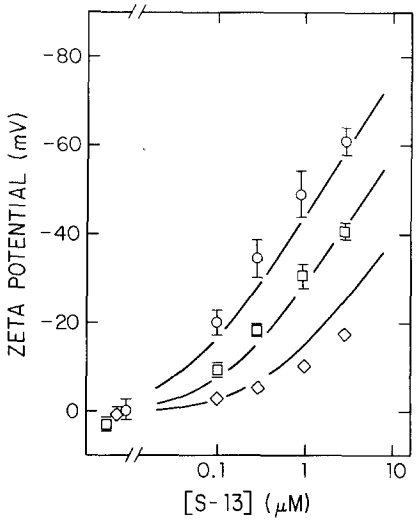

Fig. 3. A plot of the zeta potential of egg PC multilamellar vesicles as a function of the aqueous concentration of S-13. The zeta potential of the PC vesicles is zero in the absence of S-13. Adsorption of S-13 onto the vesicles produces a negative zeta potential in 0.001 M NaCl (circles), 0.01 M NaCl (squares) and 0.1 M NaCl (diamonds) solutions

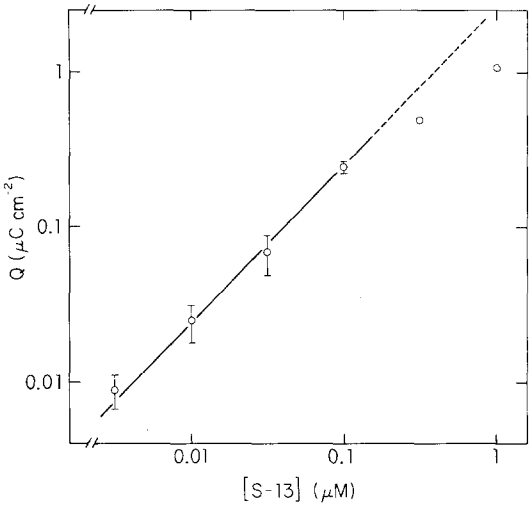

Fig. 4. The number of charges (A^- form of S-13) per unit area adsorbed onto one interface of a diphytanoyl PC/chlorodecane bilayer plotted as a function of the [S-13] at pH 8.3. The line is a least squares fit to the data when [S-13] < 0.1 μM. The adsorption coefficient is $\beta_A = 2.6\ 10^{-2}$ cm

teristic of other weak acid protonophores [5, 6, 9, 29, 47]. The deviations from the theoretical curves noted at high concentrations of S-13 in the 0.1 M NaCl solutions are presumably due to the production of electrostatic boundary potentials within the membrane, as discussed in detail elsewhere [5].

Third, we measured the adsorption coefficient of the anion onto the same diphytanoyl PC/chlorodecane membranes used for the kinetic voltage clamp measurements described below. We applied a large (200 mV) voltage clamp to the membrane and measured the current after the capacitance transient had decayed. This large voltage moves essentially all the adsorbed anions from one interface to the other side of the membrane. Thus, the integral of $I(t) - I(\infty)$ over time, where $I(t)$ is the current measured at time t after the application of the voltage clamp and $I(\infty)$ is the steady-state current, gives the number of charges per unit area adsorbed to one interface. The results obtained at pH 8.3 are illustrated in Fig. 4. The deviations from linearity that occur, when [S-13] > 0.1 μM are presumably due to the production of an electrostatic boundary potential within the membrane [5]. Using the linear region of the curves, we deduce ($\beta_A = Q/F[A^-]$) that $\beta_A = 2.6 \times 10^{-2}$ cm from the pH 8.3 data (Fig. 4) and $\beta_A = 1.6 \times 10^{-2}$ cm from the pH 9.3 data (*data not shown*). These values obtained on diphytanoyl PC/chlorodecane planar bilayer membranes agree, within a factor of two, with the values of 3×10^{-2} cm deduced from equilibrium dialysis measurement on sonicated vesicles and zeta potential measurements on multilamellar vesicles. Thus, the adsorption of the anionic form of S-13 onto the interface of PC membranes is independent of the dielectric constant of the membrane interior.

Determination of pK

We could not measure the value of β_{HA} using conventional equilibrium dialysis methods because the HA form of S-13 has a solubility of <0.1 μM in aqueous solutions [56], and this concentration of S-13 cannot be detected spectrophotometrically. However, we could determine spectrophotometrically the surface pK of S-13 adsorbed to sonicated egg PC vesicles. Our results agreed with the measurements of Bakker et al. [1]: the surface pK is about 7.0–7.3.

Determination of pK^{aq}

Wilson et al. [56] reported that the aqueous pK of S-13, pK^{aq}, is 6.4. However, their spectroscopic measurements were made in solutions containing a significant fraction of either ethanol or dimethylformamide and the pK^{aq} they reported is probably a slight overestimate. We determined pK^{aq} from conductance measurements made on diphytanoyl PC/decane membranes illustrated in Fig. 5. (The magnitude of the relaxation in the current is

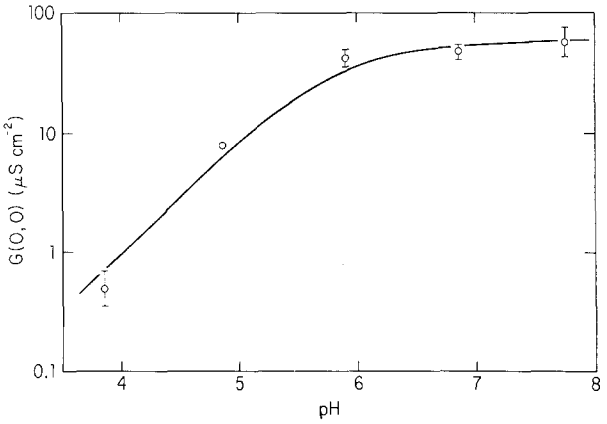

Fig. 5. The conductance of diphytanoyl PC/decane bilayers exposed to S-13 plotted as a function of pH. The solution contained 1 M NaCl, 0.1 μM S-13, 0.01 M phosphate, 0.01 M citrate and 0.01 M HEPES. The temperature was T = 20°C. The solid line is drawn with a pK^{aq} = 5.8

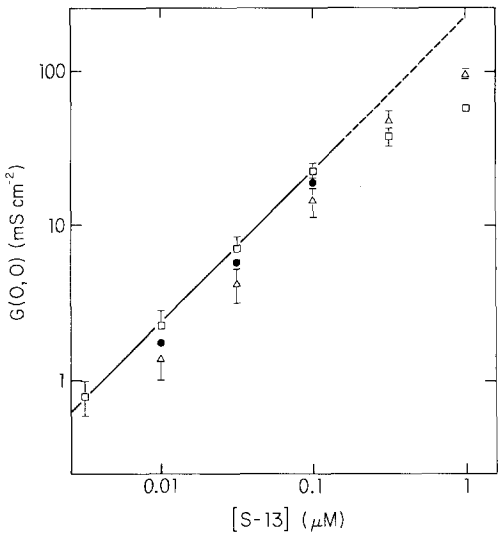

Fig. 6. A plot of the conductance of diphytanoyl PC/chlorodecane bilayers as a function of [S-13]. The triangles, squares and filled circles illustrate the data obtained at pH 7.3, 8.3 and 9.3, respectively. The straight line is a least squares best fit through the pH 8.3 data for [S-13] < 0.1 μM

negligible for membranes formed with decane: the steady state, $G(0, \infty)$, and instantaneous, $G(0, 0)$ conductances measured in the limit of zero applied voltage are essentially identical [41].) The conductance $G(0, 0)$, which is described by Eq. (12), is proportional to $[A^-]$. It should fall to $\frac{1}{2}$ the value measured in alkaline solutions with the pH = pK^{aq}. The curve in Fig. 5 is drawn assuming a pK^{aq} = 5.8. We estimate the accuracy of this determination to be about ±0.2 pK units.

Determination of k_A

If we know the value of β_A we can use Eq. (12) to deduce the value of the rate constant k_A from conductance measurements. The conductance measurements made on diphytanoyl PC/chlorodecane membranes are illustrated in Fig. 6. When [S-13] < 0.1 μM, the conductance is proportional to [S-13]. We consider only these data. The deviations at higher S-13 concentrations are presumably due to electrostatic boundary potentials [5, 29]. If we take $G(0, 0)/[A^-]$ from the conductance data obtained at pH 8.3 (Fig. 6) and use the value of $\beta_A = 2.6 \times 10^{-2}$ cm, the value obtained on the same membranes (Fig. 4), we obtain $k_A = 2.4 \times 10^3$ sec^{-1}. If we take $G(0, 0)/[A^{-1}]$ from the data obtained at pH 9.3 (Fig. 6) and use the value of $\beta_A = 1.6 \times 10^{-2}$ cm obtained on the same membranes, we obtain a similar value for the rate constant, $k_A = 3.2 \times 10^3$ sec^{-1}. Note from a comparison of the data in Figs. 5 and 6 that the conductance and rate constant k_A are several orders of magnitude higher on PC/chlorodecane membranes than on PC/decane membranes. This difference is due mainly to the different dielectric constants of the two membranes (2.7 *vs.* 2.1 [10]), which affects the Born energy required to partition an anion into a medium of low dielectric constant. We argue elsewhere that PC/chlorodecane membranes provide a good model for studying ion transport through the inner mitochondrial membrane, which contains a high concentration of integral proteins [5, 37].

Determination of P_{HA}, β_{HA}, and k_{HA}

We deduce a value for the rate constant k_{HA} using a technique developed by LeBlanc [34]. As discussed in detail by McLaughlin and Dilger [37], the membrane potential produced by a difference in the pH of the solutions on the two sides of the membrane is Nernstian when the mechanism illustrated in Fig. 1 is operative. As the pH of the aqueous solutions increases, however, the back diffusion of HA becomes rate limiting and S-13 behaves as a lipid soluble anion. In this limit $dV/d\text{pH} = 0$. Thus by measuring $dV/d\text{pH}$ as a function of pH we can obtain a value for the permeability of the membrane to HA, P_{HA}, from Eq. (19):

$$dV/d\text{pH} = \frac{2.303(RT/F)[H^+]K^{aq}(1 + 2\delta P_{HA}/D)}{(1 + [H^+]K^{aq}(1 + 2\delta P_{HA}/D))}. \quad (19)$$

In this equation $D/2\delta$ is the permeability of the two

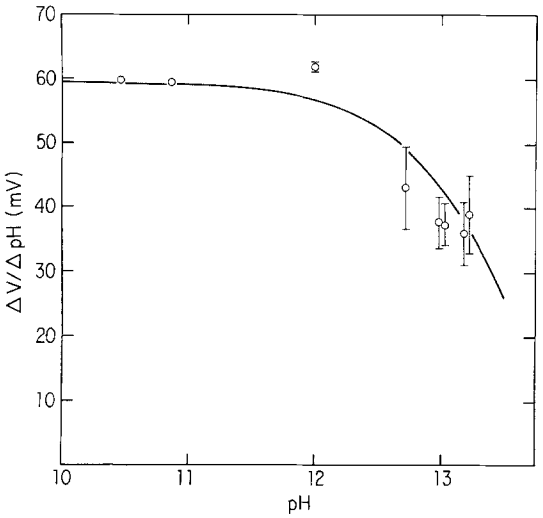

Fig. 7. A plot of the membrane potentials induced by pH gradients in the presence of 0.1 μM S-13 on each side of a diphytanoyl PC/decane membrane. The theoretical curves is from Eq. (19) assuming that the permeability of the membrane to HA is P_{HA} = 10^4 cm sec^{-1}. The membrane potential is Nernstian for pH < 12. The vertical lines illustrate the standard deviations in the membrane potential obtained from at least three different experiments

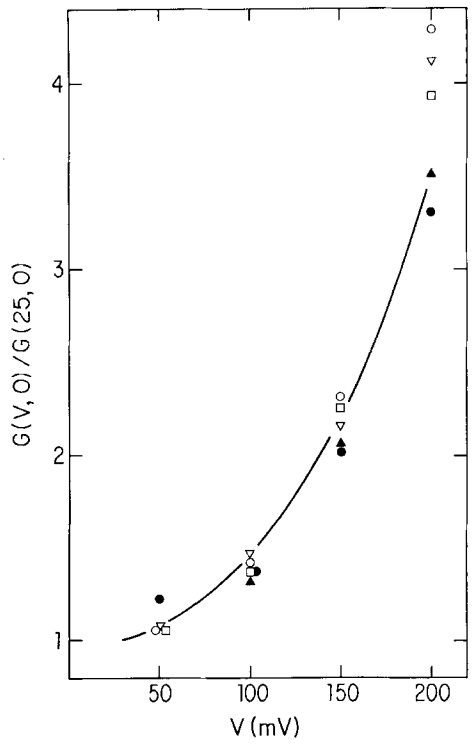

Fig. 8. Conductance-voltage curves for diphytanoyl PC/chlorodecane membranes exposed to S-13. The initial conductance, $G(V, 0)$ was measured as a function of voltage, V. $G(V, 0)$ is divided by the initial conductance at 25 mV, $G(25, 0)$ then plotted against the applied voltage: pH 7.3, [S-13] = 0.03 μM (open circles); pH 7.3, [S-13] = 0.1 μM (filled circles); pH 8.3, [S-13] = 0.01 μM (inverted triangles); pH 8.3, [S-13] = 0.03 μM (squares); pH 8.3, [S-13] = 0.1 μM (filled triangles). The data points represent average values for at least four membranes

unstirred layers to HA, δ is the thickness of the unstirred layers (about 10^{-2} cm in our chamber [6]), D is the diffusion coefficient of the HA and A^- species of S-13 in the aqueous phases, which we assume to be 5×10^{-6} cm^2/sec, and K^{aq} is the association constant of S-13 in the aqueous phase ($K^{aq} = 6 \times 10^5$ M^{-1} or $pK^{aq} = 5.8$; *see* Fig. 5). Figure 7 illustrates that for pH < 12, dV/dpH has a Nernstian value of 60 mV/decade; when pH > 12, the value of dV/dpH is <60 mV/decade. For pH 13, dV/dpH = 40 mV/decade. The curve in Fig. 7 illustrates the results are consistent with a value of $P_{HA} = 10^4$ cm/sec. The value of P_{HA} we obtain from the membrane potential experiments represents the permeability of the entire membrane to HA [37].

We can calculate a value for k_{HA} if there are no interfacial barriers for HA ($k_{HA} = P_{HA}/\beta_{HA}$). Since $\beta_A/\beta_{HA} = K/K^{aq}$, $k_{HA} = P_{HA}K/K^{aq}\beta_A$. If $7.0 < pK < 7.3$, it follows from $\beta_A \sim 2 \times 10^{-2}$ cm, $pK^{aq} = 5.8$ that $3 \times 10^{-1} < \beta_{HA} < 6 \times 10^{-1}$ cm and that $k_{HA} = 1.5 \times 10^4$–3×10^4 sec^{-1}. We cannot place great confidence in the value of k_{HA} determined from this measurement. The data illustrated in Fig. 7 are difficult to obtain at pH 13, and the interpretation is complicated because we cannot measure the adsorption coefficient of the HA species directly.

We now deduce the parameters required to describe the model illustrated in Fig. 1 from kinetic voltage clamp and charge pulse measurements.

Voltage-Clamp Results

Barrier Shape

Figure 8 illustrates the dependence of conductance, $G(V, 0)$, on the applied voltage, V. The model predicts that the shapes of the $G(V, 0)/G(0, 0)$ *vs.* V curves should be independent of both [S-13] and pH; our experimental results agree qualitatively with this prediction. From Eqs. (5), (8) and (9) it follows that:

$$G(V, 0)/G(0, 0) = b \sinh(u/2)/\sinh(bu/2). \quad (20)$$

The curve in Fig. 8 is drawn according to Eq. (20) with $b = 0.5$. In other words, the data are described by assuming that the A^- species encounters a trapezoidal barrier whose minor base spans $\frac{1}{2}$ the width of the membrane.

Kinetic Voltage-Clamp Measurements

The kinetic voltage-clamp and charge-pulse measurements we obtained with S-13 are similar to the results obtained with FCCP [5]; sample experimental records were illustrated previously and are not reported here for S-13. We first analyze the voltage-clamp results by assuming that the interfacial reactions illustrated in Fig. 1 are at equilibrium throughout the relaxations. It is apparent from Eq. (7) that when $K[H^+] \ll 1$ and $2k_{HA}K[H^+] \ll k'_A + k''_A$, we can deduce the value of k_A from the value of the time constant, $\tau = 1/\lambda$ measured at low applied voltage. In this case Eq. (7) reduces to $k_A \simeq 1/2\tau$. Figure 9*a* illustrates that the time constant measured at 25 mV (triangles) is independent of [S-13] for [S-13] < 0.1 μM. The average value of the time constant is about 100 μsec at pH 8.3 (Fig. 9*a*) and pH 9.3 (*data not shown*). Thus Eq. (7) gives a value of $k_A = 4 \times 10^3$ sec^{-1} from the time constants measured at alkaline pH values. This value agrees, within a factor of two, with the value for k_A deduced from the independent measurements ($k_A = 2.4 \times 10^3$–3.2×10^3 sec^{-1}, *see above*).

Equation 6 illustrates that if we know the value of the rate constant for the movement of the anion, k_A, we can obtain a value for the product of the equilibrium association constant and the rate constant for the movement of the neutral species, Kk_{HA}, by measuring the magnitude of the relaxation. Figure 9*b* illustrates that the magnitude of the relaxation recorded at low voltage (25 mV, triangles) is indeed independent of the [S-13] for [S-13] < 0.1 μM, as required by the model; the value of α is 5. If we take a value of $k_A = 4 \times 10^3$ sec^{-1} we obtain a value of $Kk_{HA} = 2\ 10^{11}$ M^{-1} sec^{-1}. If $K = 10^7$ M^{-1}, the value we obtain from spectroscopic measurements, $k_{HA} = 2 \times 10^4$ sec^{-1}. This agrees with the value we obtained from steady-state membrane potential experiments, $1.5 \times 10^4 < k_{HA} < 3 \times 10^4$ sec^{-1}.

The theoretical and experimental dependence of the time constant of the relaxation on voltage and pH is illustrated in Fig. 10*a*. We consider the fit to be acceptable.

The model that assumes the interfacial reactions illustrated in Fig. 1 remain at equilibrium ["equilibrium model," *see* Eq. (6)] predicts that α should decrease 10-fold for every unit decrease in the pH. Between pH 8.3 and 7.3, this prediction is qualitatively confirmed[5] by the data illustrated in Fig. 10*b*. However, Fig. 11 illustrates that as the pH is lowered below pH 7.3, α does not decrease as rapidly with pH as predicted by the equilibrium model. The solid line in Fig. 11 is the prediction of the equilibrium model and the dashed line is the theoretical prediction of a more general model[6] that assumes the interfacial reactions in Fig. 1*a* and *c* operate in parallel with diffusion limited rate constants. The results illustrated in Fig. 11 are consistent with the notion that the reaction of OH^- with

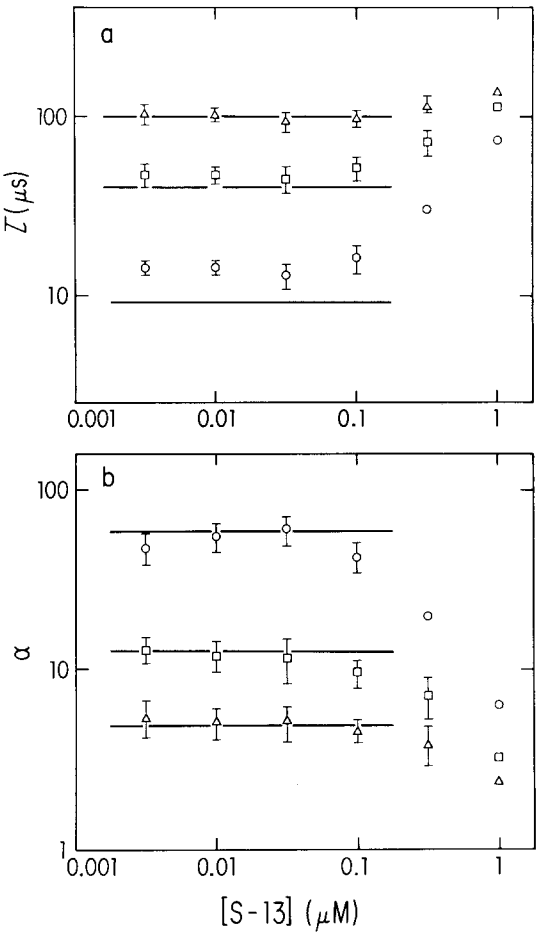

Fig. 9. The time constant, τ, and the amplitude, α, of the relaxations in the current observed in voltage-clamp experiments. The data are plotted as a function of [S-13] on a log-log scale. The triangles, squares and circles represent the results obtained at 25, 100 and 200 mV, respectively, for pH 8.3. The lines through the data illustrate the predictions of the model when $k_A = 4 \times 10^3$ sec^{-1}, $k_{HA} = 2 \times 10^4$ sec^{-1}, pK = 7.0 and $b = 0.5$

[5] However, α should increase 10-fold when the pH increases from 8.3 to 9.3; we observed only a fivefold increase (*data not shown*). We do not understand the reason for this slight deviation from the prediction of the model at high pH.

[6] We solved the equations that describe the general model illustrated in Fig. 1: we assumed the interfacial reactions illustrated in Fig. 1 occur in parallel and are not necessarily at equilibrium. Outlines of both the equations and a computer program that solves them are available upon request.

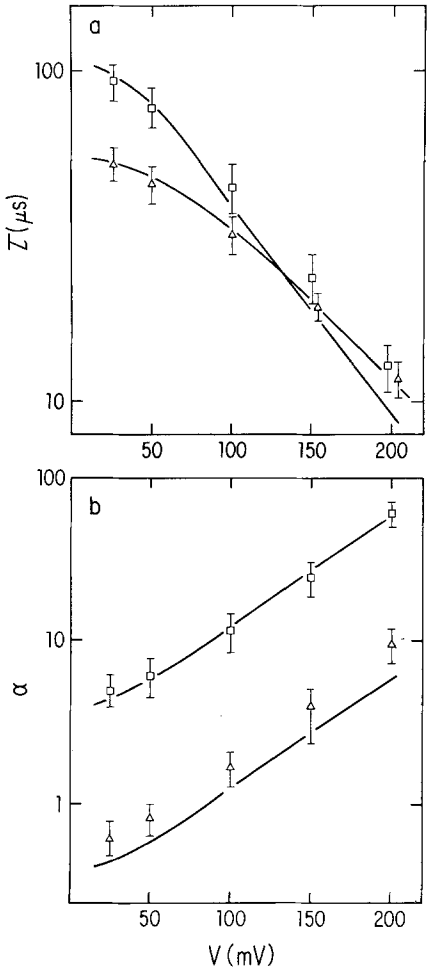

Fig. 10. The dependence of the time constant, τ, and amplitude, α, on pH and voltage; the scales for τ and α are logarithmic. The triangles and squares illustrate the results obtained when the [S-13] = 0.03 μM at pH 7.3 and 8.3, respectively. The lines through the data illustrate the predictions of the model when $k_A = 4 \times 10^3$ sec^{-1}, $k_{HA} = 2 \times 10^4$ sec^{-1}, pK = 7.0 and $b = 0.5$

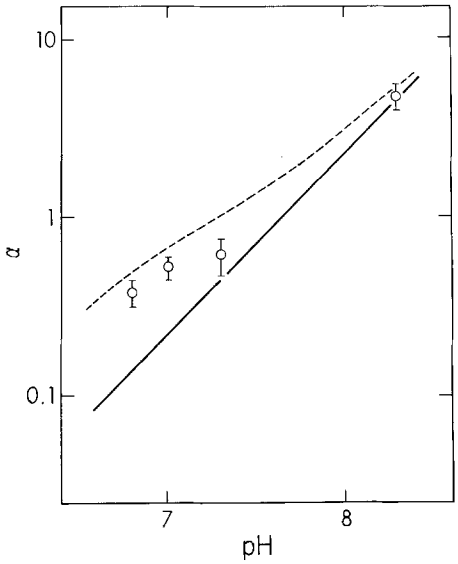

Fig. 11. The dependence of the amplitude, α, on pH; the scale for α is logarithmic. The solid line illustrates the theoretical prediction if we assume the interfacial reactions in Fig. 1 remain at equilibrium [Eq. (6)]. The dashed line illustrates the prediction if we assume that the mechanisms illustrated in Fig. 1*a* and *c* operate in parallel, that $k_R = k_4 = 10^{11}$ M^{-1} sec^{-1}, the diffusion-limited values in a bulk aqueous phase, and $k_1 = k_2 = 0$. To calculate both curves, we assumed that $k_A = 4 \times 10^3$ sec^{-1}, $k_{HA} = 2 \times 10^4$ sec^{-1}, pK = 7.0 and $b = 0.5$. The applied voltage was 25 mV

adsorbed HA illustrated in Fig. 1*c* becomes rate limiting for pH < 7.3.

Charge Pulse Measurements

The decay of the voltage following a charge pulse of 50 nsec duration could always be described by assuming that there are only two exponential relaxation processes.

We can obtain estimates of K_A, K_{HA} and N_o from data obtained at a single pH if we assume, as a first approximation, that the interfacial reactions remain at equilibrium[7] [Eqs. (14)–(18)]. Table 1 shows the results of charge pulse relaxation measurements made on membranes of different composition. The time constant τ_2 and the amplitudes of the relaxations, as well as K_A and K_{HA}, depend on pH, whereas N_o and τ_1 are essentially independent of pH as predicted theoretically.

The values of k_{HA} and the surface pK may be obtained by fitting K_{HA} as a function of pH to these two parameters. We consider the charge pulse data when pH > 7.3, and assume the protonation reactions at the interfaces are in equilibrium. Equation (17) provides a reasonable fit to the data in Table 1 if we assume that $k_{HA} = 2.9 \times 10^4$ sec^{-1} and pK = 7.3 for the PC membranes and that $k_{HA} = 1.3 \times 10^4$ sec^{-1}, pK = 8.3 for PC : PG membranes. The surface pK of 7.3 obtained from these kinetic measurements on planar PC/chlorodecane membranes agrees with the value obtained from spectroscopic measurements on sonicated PC vesicles (7.0 < pK < 7.3, *see above*). The electrostatic surface potential of a PC membrane is zero; the surface potential of a 1 : 1 PC : PG membrane in 0.1 M NaCl is about −60 mV [13, *unpublished data*]. Thus, we expect the surface pK of S-13 on the PC : PG membranes to be one pH unit more alkaline than on a PC membrane. This prediction agrees with the experimental observation. We estimated the values of k_A for the PC and the PC : PG membranes from the data at pH > 8.3, using Eq. (18). We determined that $k_A = 5 \times 10^3$ and 6×10^3 sec^{-1} for the PC and PC : PG mem-

[7] The calculated values for K_A, K_{HA} and N_o in Table 1 for the PC membranes are only valid for pH > 7.3. For pH < 7.3, a nonequilibrium model[6] should be used.

Table 1. Charge pulse relaxation data from PC/chlorodecane, PE/chlorodecane and 1 : 1 PC : PG/chlorodecane lipid bilayer membranes

pH	τ_1 (μsec)	τ_2 (μsec)	a_2	K_{HA} (sec^{-1})	K_A (sec^{-1})	N_o (pmol cm^{-2})
			PC Membranes			
6.3	20 ± 2.3	79 ± 16	0.93 ± 0.019	21000 ± 3100	2900 ± 430	2.2 ± 0.32
6.7	18 ± 1.8	53 ± 9.3	0.80 ± 0.085	20000 ± 1800	3900 ± 340	2.8 ± 0.41
7.0	15 ± 1.3	41 ± 12	0.52 ± 0.11	18000 ± 2200	4700 ± 480	3.9 ± 0.85
7.3	16 ± 1.9	51 ± 8.5	0.45 ± 0.12	14000 ± 2100	5100 ± 660	3.5 ± 0.63
7.7	17 ± 1.2	73 ± 16	0.29 ± 0.053	8800 ± 850	4800 ± 470	4.1 ± 0.37
8.0	16 ± 1.1	110 ± 21	0.25 ± 0.075	5900 ± 290	5300 ± 380	3.8 ± 0.71
8.3	18 ± 1.7	210 ± 29	0.20 ± 0.063	2900 ± 380	4500 ± 520	4.2 ± 1.1
8.7	17 ± 2.5	650 ± 78	0.20 ± 0.043	950 ± 180	5300 ± 680	3.6 ± 0.75
9.0	18 ± 2.1	1100 ± 180	0.19 ± 0.054	580 ± 110	5500 ± 550	3.5 ± 0.61
9.3	19 ± 2.8	2000 ± 160	0.18 ± 0.061	310 ± 48	4900 ± 420	4.0 ± 0.58
			PE Membranes			
6.5	6.7 ± 0.91	41 ± 9.7	0.97 ± 0.010	64000 ± 7100	7100 ± 1300	1.5 ± 0.9
7.0	8.8 ± 0.97	41 ± 9.0	0.86 ± 0.032	39000 ± 3100	13000 ± 1800	1.1 ± 0.2
7.5	7.4 ± 0.42	30 ± 2.3	0.39 ± 0.037	24000 ± 1000	13000 ± 700	2.8 ± 0.4
8.0	10 ± 1.2	56 ± 8.2	0.53 ± 0.060	16000 ± 700	14000 ± 2000	1.5 ± 0.3
8.5	7.6 ± 0.46	59 ± 6.0	0.30 ± 0.041	11000 ± 600	14000 ± 1200	2.6 ± 0.5
9.0	6.6 ± 0.81	97 ± 9.5	0.27 ± 0.047	6900 ± 300	17000 ± 1700	2.6 ± 0.6
			PC : PG Membranes			
7.7	31 ± 6	300 ± 110	0.91 ± 0.028	9300 ± 710	5700 ± 1600	0.44 ± 0.16
8.3	39 ± 8	470 ± 120	0.89 ± 0.025	6100 ± 930	5800 ± 1600	0.33 ± 0.09
8.7	51 ± 3	700 ± 140	0.85 ± 0.010	3500 ± 450	5000 ± 370	0.35 ± 0.06
9.3	69 ± 8	3400 ± 450	0.90 ± 0.008	1300 ± 140	5300 ± 910	0.14 ± 0.02
9.6	79 ± 23	5700 ± 1400	0.83 ± 0.043	510 ± 38	5000 ± 1300	0.17 ± 0.05
10	69 ± 19	11000 ± 1100	0.86 ± 0.001	320 ± 30	6000 ± 1100	0.13 ± 0.01

Table 2. Concentration dependence of charge pulse relaxation data from PC/chlorodecane and PE/chlorodecane bilayer membranes

[S-13] (nM)	τ_1 (μsec)	τ_2 (μsec)	a_2	K_{HA} (sec^{-1})	K_A (sec^{-1})	N_o (pmol cm^{-2})	β_o (10^{-2} cm)
			PC Membranes (pH 8)				
3	44 ± 8.3	1300 ± 250	0.96 ± 0.033	4900 ± 960	5400 ± 1100	0.13 ± 0.025	2.2
10	42 ± 5.3	470 ± 56	0.89 ± 0.040	5600 ± 490	5000 ± 720	0.38 ± 0.062	1.9
30	31 ± 3.8	200 ± 19	0.63 ± 0.12	5300 ± 680	5800 ± 840	1.1 ± 0.25	1.8
100	16 ± 1.1	110 ± 21	0.25 ± 0.075	5900 ± 290	5300 ± 380	3.8 ± 0.71	1.9
300	9.3 ± 1.7	95 ± 22	0.15 ± 0.037	6200 ± 340	6300 ± 450	5.6 ± 1.4	0.93
			PE Membranes (pH 7.5)				
3	15 ± 2.4	820 ± 200	0.98 ± 0.004	20000 ± 2700	15000 ± 3900	0.065 ± 0.025	1.1
10	12 ± 0.7	260 ± 39	0.96 ± 0.007	22000 ± 500	17000 ± 1900	0.15 ± 0.020	0.75
30	11 ± 0.6	97 ± 20	0.86 ± 0.036	22000 ± 600	17000 ± 1400	0.47 ± 0.13	0.78
100	7.4 ± 0.42	30 ± 2.3	0.39 ± 0.037	24000 ± 1000	13000 ± 700	2.8 ± 0.4	1.4
300	5.1 ± 0.57	25 ± 2.2	0.27 ± 0.029	25000 ± 1400	15000 ± 500	4.1 ± 0.6	0.68

branes, respectively. We attempted to fit the data obtained from PE/chlorodecane membranes only for pH < 8; when pH > 8 the amine group is deprotonated, the membrane acquires a negative charge and the interpretation of the data is complex [48, 52]. We assumed that the surface pK was 7.3 and obtained $k_{HA} = 6.5 \times 10^4$ sec^{-1} and $k_A = 1.5 \times 10^4$ sec^{-1}. Table 2 contains the results of charge pulse experiments on PC/chlorodecane or PE/chlorodecane membranes at pH 8 or 7.5, respectively. The time constants and amplitudes of the two relaxations depend markedly on the concentration of S-13. For example, the time constant τ_2 decreases more than an order of magnitude when [S-13] increases from 3 to 300 nM. However, the rate constants K_{HA} and K_A and the partition coefficient $\beta_o = N_o/2[S\text{-}13]$ are approximately independent of protonophore concentration for [S-13] < 0.1 μM. The

Table 3. Buffer dependence of charge pulse relaxation data from PC/chlorodecane, and from PE/chlorodecane bilayer membranes at pH 8

Buffer	τ_1 (μsec)	τ_2 (μsec)	a_2	K_{HA} (sec^{-1})	K_A (sec^{-1})	N_o (pmol cm^{-2})
			PC Membranes			
HEPES (7.5)	18 ± 2.1	110 ± 17	0.28 ± 0.063	6100 ± 710	4900 ± 620	3.6 ± 0.58
Bicine (8.3)	15 ± 1.6	120 ± 18	0.23 ± 0.028	5200 ± 620	5700 ± 590	4.0 ± 0.62
EPPS (8.0)	17 ± 1.9	120 ± 14	0.27 ± 0.038	5500 ± 510	5300 ± 720	3.5 ± 0.66
			PE Membranes			
HEPES (7.5)	7.5 ± 0.42	43 ± 2.3	0.31 ± 0.027	16000 ± 400	13000 ± 1200	2.9 ± 0.3
Tricine (8.2)	6.3 ± 0.17	44 ± 2.6	0.30 ± 0.016	15000 ± 600	16000 ± 600	2.7 ± 0.2
Tris (8.3)	8.0 ± 1.1	43 ± 5.0	0.33 ± 0.063	16000 ± 800	12000 ± 500	2.8 ± 0.6

Table 4. Buffer dependence of charge pulse relaxation data from 1 : 1 PC : PG/chlorodecane bilayer membranes at pH 9.3

Buffer	τ_1 (μsec)	τ_2 (μsec)	a_2	K_{HA} (sec^{-1})	K_A (sec^{-1})	N_o (pmol cm^{-2})
Bicine (10 mM)	69 ± 8	3.4 ± 0.45	0.90 ± 0.010	1300 ± 140	5300 ± 900	0.14 ± 0.02
Triphosphate (10 mM)	77 ± 7	3.1 ± 0.4	0.89 ± 0.012	1300 ± 180	4600 ± 640	0.13 ± 0.02
Triphosphate (1 mM)	80 ± 25	2.9 ± 0.5	0.88 ± 0.020	1200 ± 180	4800 ± 1800	0.15 ± 0.03
Tetraphosphate (1 mM)	78 ± 21	3.0 ± 0.8	0.87 ± 0.035	1200 ± 240	5000 ± 1400	0.15 ± 0.04
Triphosphate (1 mM, CO_2 removed)	78 ± 3	2.7 ± 0.6	0.88 ± 0.010	1400 ± 60	4500 ± 330	0.16 ± 0.02

result is consistent with our model, which assumes that the protonophore molecules act independently. The results of the charge pulse and voltage-clamp experiments are in good agreement.

We noted previously that if the mechanism illustrated in Fig. 1*a* operates alone to transport protons across the membrane, the value of k_R is anomalously high for FCCP [5]. The anomaly is even greater for S-13 (Appendix I). One possible explanation is that the buffer from the aqueous phase delivers the proton directly to the adsorbed anion, as illustrated in Fig. 1*b*. To test this hypothesis we performed charge pulse measurements using different anionic, cationic and zwitterionic buffers. The results of these experiments are summarized in Table 3. The charge and chemical nature of the buffer influenced neither the relaxation data nor the rate constants K_{HA} and K_A. Furthermore, the data were not affected when we lowered the concentration of the buffer to 10^{-3} M (*data not shown*). (It is difficult to interpret the data obtained at buffer concentrations $<10^{-3}$ M because of diffusion polarization in the aqueous unstirred layers[8].) These experiments, however, do not rule out the possibility that all these buffers transfer protons to S-13 with a rate constant $>10^8$ M^{-1} sec^{-1}. To test this possibility, we performed kinetic experiments on negatively charged membranes using a polyanionic buffer. If the bulk concentration of either triphosphate or tetraphosphate is 10^{-3} M, the concentration of these anionic buffers at the membrane-solution interface, where the surface potential is −60 mV, should be less than 1 μM according to the Boltzmann relationship. We could not make voltage-clamp measurements because the relaxations were too fast to obtain accurate data with PC : PG membranes in 0.1 M NaCl. However, we could obtain good data with charge pulse measurements (Table 4). In one series of experiments we degassed the water and bubbled either argon or nitrogen through the aqueous solutions to avoid the production of a significant concentration of carbonic acid in the solution. The relaxations were not not affected by these procedures (Table 4). Thus, we believe we have prevented any significant direct transfer of the proton from the buffer to the adsorbed anionic form of S-13 in these experiments. If the mechanism illustrated in Fig. 1*b* were operative, we should have observed an order of magnitude increase in the value of τ_2 and other changes in the relaxation data. The absence of these changes argues that the mechanism illustrated in Fig. 1*b*, even operating in conjuction with the mechanism in Fig. 1*a*, cannot account for the ability of

[8] *See* footnote 3, p. 75.

Table 5. Comparison between different linear uncouplers for PC/chlordecane membranes

Uncoupler	β_A (cm)	β_{HA} (cm)	P_{HA} (cm sec^{-1})	k_A (sec^{-1})	k_{HA} (sec^{-1})
CCCP	2×10^{-3}	2×10^{-3}	20	2×10^{2}	5×10^{3}
FCCP	3×10^{-3}	3×10^{-3}	50	8×10^{2}	10^{4}
S-13	2×10^{-2}	5×10^{-1}	10^{4}	4×10^{3}	2×10^{4}

CCCP data taken from Kasianowicz et al. [29], FCCP data taken from Benz and McLaughlin [5], and the S-13 data taken from this study.

protons to cross the membrane solution interface.

The results of our charge pulse experiments are qualitatively consistent with the hydrolysis mechanism (Fig. 1*c*). For example, the equilibrium model predicts that K_A should decrease an order of magnitude when the pH is decreased from 9.3 to 6.3. However, the calculated values of K_A for PC membranes (Table 1) remain constant over this pH range, as predicted by a nonequilibrium model[9].

Discussion

Proton Transport Across the Interior of the Membrane

The simple kinetic scheme illustrated in Fig. 1 describes the mechanism by which the weak acids FCCP [5], CCCP [29, 43] and S-13 transport protons across the interior of a bilayer membrane. The adsorption and kinetic parameters we deduce for these three protonophores are listed in Table 5. Note that the A^- and HA forms of the weak acids adsorb strongly to the membrane-solution interface. The values of β_A and β_{HA} are all $>2 \times 10^{-3}$ cm. If we assume the thickness of the interfacial region is 0.5 nm, the dimensionless partition coefficients into the interfacial region from the aqueous phase are $>10^4$. The partition coefficient of the anion into the hydrocarbon interior of the membrane from the aqueous phase, which can be calculated from the measured value of the conductance, is of order 1 for the A^- form of CCCP [29] and FCCP [5] and of order 10 for S-13. Thus the anions partition favorably into the interior of the membrane. Since the rate-limiting step for the cycle illustrated in Fig. 1 is the movement of the anion (Table 5, pH = pK), the favorable partitioning of the anions into the membrane interior explains why these weak acids are such efficient protonophores.

We have described elsewhere the carrier mechanism illustrated in Fig. 1 [5, 37]. In brief, the application of a voltage moves anions from the free energy well at the left-hand interface to the well at the right-hand interface. The concentration of A^- increases at the right-hand interface and the reactions illustrated in Fig. 1, which remain at equilibrium for pH > 7.3, produce HA and increase proportionally the concentration of HA at the right-hand interface. HA diffuses back to the left-hand interface rather than moving into the right-hand aqueous phase.

It is not necessary to postulate that an interfacial barrier prevents HA from moving into the aqueous phase adjacent to the membrane. The permeability of the aqueous unstirred layer adjacent to the membrane is $D/\delta = 5 \times 10^{-4}$ cm sec^{-1}, where D is the aqueous diffusion coefficient and δ is the thickness of the unstirred layer. Table 5 illustrates that the permeability of the entire membrane to HA, P_{HA}, is many orders of magnitude higher than this value for all three protonophores. Furthermore, our steady-state measurements of P_{HA} agree with our kinetic measurements of the permeability of the interior of the membrane to HA, $\beta_{HA}k_{HA}$ (Table 5). This demonstrates experimentally that interfacial barriers do not exist for the HA form of these three protonophores.

The carrier mechanism is slightly more complicated for S-13 than for CCCP and FCCP because the surface pK is not equal to the bulk pK ($\beta_A \neq \beta_{HA}$). Nevertheless, the parameters derived from our kinetic measurements using the simple carrier model illustrated in Fig. 1 and the parameters determined by direct independent measurements agree within a factor of two. Although the carrier model is oversimplified, the results we obtained with FCCP, CCCP and S-13 argue strongly that it captures the essential features of the transport mechanism within the membrane. This suggests we can use this model and the S-13 data to address the question of how protons cross the membrane-solution interface.

Membrane-Solution Interface

The simplest mechanism by which protons could cross the membrane-solution interface is illustrated in Fig. 1*a*. As we discuss in Appendix I, the value of k_R required to explain our experimental data with this mechanism is $k_R > 10^{13}$ M^{-1} sec^{-1}, a value two orders of magnitude higher than the fastest diffusion-limited reaction in a bulk aqueous solution. In view of the fact that Nachliel and Gutman [40] have shown the diffusion coefficient of protons in the wa-

[9] *See* footnote 6, p. 75.

ter adjacent to surfaces is not anomalously fast this scheme must be considered unlikely.[10]

We now consider the mechanism illustrated in Fig. 1*b*, which could account for the data obtained with neutral membranes if buffers transfer protons directly to the adsorbed anions with a rate constant $>10^8$ M^{-1} sec^{-1}. All "normal" weak acids exchange protons with rate constants of this order in a bulk aqueous phase [4, 12] and Gutman [20] showed that such reactions can also occur at the membrane-solution interface. However, our experiments with negative membranes demonstrate that there must be at least one additional mechanism that delivers protons to the anion. When we reduced the buffer concentration at the membrane-solution interface to <1 μM, which is too low to provide a sufficient collisional transfer of protons to adsorbed anions, the kinetic parameters were unchanged (Table 4). It seems likely to us that protons are transferred directly from water to the anion, as illustrated in Fig. 1*c*. This mechanism occurs with most weak acids in bulk aqueous phases, as discussed in detail by Eigen [11].

Biological Implications

All known protonophores uncouple oxidation from phosphorylation. This result is consistent with the chemiosmotic hypothesis but it is difficult to explain in terms of the chemical hypothesis. Protonophores are also useful for distinguishing between the chemiosmotic hypothesis, in which oxidation is coupled to phosphorylation by means of a $\Delta\tilde{\mu}_{H^+}$, and some versions of local chemiosmosis that have been proposed. For example, Kell [32] argued that protons move parallel to the bilayer component of the membrane and do not equilibrate with the bulk aqueous phase because the Stern layer (inner part of the electrostatic aqueous diffuse double layer, thickness <1 nm) immediately adjacent to the membrane exerts a high resistance to their perpendicular movement. Our measurements contradict this argument. Protons crossing the aqueous phase adjacent to the membrane encounter no high resistance. They are transferred very rapidly in either the absence or presence of fixed charges and Stern layers. Our results with protonophores agree with experimental results using a laser-pulse proton jump technique: protons from the membrane equilibrate extremely rapidly with the aqueous phase [40]. These results argue against local chemiosmosis mechanisms that allow the proton to contact water molecules at any time in their cycle. It is difficult (but not impossible) to construct a local chemiosmosis model that satisfies this criterion and also allows protons from the aqueous phase to couple oxidation to phosporylation.

This work was supported by National Science Foundation grant PCM 8340253 to Dr. McLaughlin and Deutsche Forschungsgemeinschaft grant Be865/3-1 and Nato grant 264-82 to Dr. Benz. We thank Dr. J. Nagle for helpful comments.

[10] *See* footnote, 2, p. 74.

References

1. Bakker, E.P., Arents, J.P., Hoebe, J.P.M., Terada, H. 1975. Surface potential and the interaction of weakly acidic uncouplers of oxidative phosphorylation with liposomes and mitochondria. *Biochim. Biophys. Acta* **387**:491–506
2. Bangham, A.D., Hill, M.W., Miller, N.G.A. 1974. Preparation and use of liposomes as models of biological membranes. *Methods Membr. Biol.* **1**:1–68
3. Barenholz, Y., Gibbes, D., Littman, B.J., Goll, J., Thompson, T.E. 1977. A simple method for the preparation of homogeneous phospholipid vesicles. *Biochemistry* **16**:2806–2810
4. Bell, R.P. 1973. The Proton in Chemistry. Cornell University Press, Ithaca
5. Benz, R., McLaughlin, S. 1983. The molecular mechanism of action of the proton ionophore FCCP (carbonylcyanide *p*-trifluoromethoxyphenylhydrazone). *Biophys. J.* **41**:381–398
6. Cohen, F.S., Eisenberg, M., McLaughlin, S. 1977. The kinetic mechanism of action of an uncoupler of oxidative phosphorylation. *J. Membrane. Biol.* **37**:361–396
7. Delahay, P. 1954. New Instrumental Methods in Electrochemistry. pp. 87–95. Interscience, New York
8. Dijk, C. van, Levie, R. de 1985. An experimental comparison between the continuum and single jump descriptions of nonactin-mediated potassium transport through lipid membranes. *Biophys. J.* **48**:125–136
9. Dilger, J., McLaughlin, S. 1979. Proton transport through membranes induced by weak acids: A study of two substituted benzimidazoles. *J. Membrane Biol.* **46**:359–384
10. Dilger, J.P., Benz, R. 1985. Optical and electrical properties of thin monoolein lipid bilayers. *J. Membrane Biol.* **85**:181–189
11. Eigen, M. 1964. Proton Transfer, Acid-Base Catalysis, and Enzymatic Hydrolysis: part I. Elementary Processes. *Ange. Chem. Int. Ed. Engl.* **3**:1–72
12. Eigen, M., Kruse, W., Maass, G., De Maeyer, L. 1964. Rate constants of protolytic reactions in aqueous solution. *Prog. React. Kinet.* **2**:287–318
13. Eisenberg, M., Gresalfi, T., Riccio, T., McLaughlin, S. 1979. Adsorption of monovalent cations to bilayer membranes containing negative phospholipids. *Biochemistry* **18**:5213–5223
14. Everitt, C.T., Redwood, W.R., Haydon, D.A. 1969. Problem of boundary layers in the exchange diffusion of water across bimolecular lipid membranes. *J. Theor. Biol.* **22**:20–32
15. Finkelstein, A., Cass, A. 1968. Permeability and electrical properties of thin lipid membranes. *J. Gen. Physiol.* **52**:145*s*–172*s*
16. Flewelling, R.F., Hubbell, W.L. 1986. Hydrophobic ion interactions with membranes: Thermodynamic analysis of te-

traphenylphosphonium binding to vesicles. *Biophys. J.* **49:**531–540
17. Flewelling, R.F., Hubbell, W.L. 1986. The membrane dipole potential in a self-consistent total membrane potential model. *Biophys. J.* **49:**541–552
18. Gupte, S., Wu, E.-S., Hoechli, L., Hoechli, M., Jacobson, K., Sowers, A.E., Hackenbrock, C.R. 1984. Relationship between lateral diffusion, collision frequency, and electron transfer of mitochondrial inner membrane oxidation-reduction components. *Proc. Natl. Acad. Sci. USA* **81:** 2606–2610
19. Gutknecht, J., Tosteson, D.C. 1973. Diffusion of weak acids across lipid bilayer membranes: Effects of chemical reactions in the unstirred layers. *Science* **182:**1258–1261
20. Gutman, M. 1984. The pH jump: Probing of macromolecules and solutions by a laser-induced, ultrashort proton pulse-theory and applications in biochemistry. *Methods Biochem. Anal.* **30:**1–103
21. Hall, J.E., Meed, C.A., Szabo, G. 1973. A barrier model for current flow in lipid bilayer membranes. *J. Membrane Biol.* **11:**75–97
22. Hanstein, W.G., Hatefi, Y. 1974. Characterization and localization of mitochondrial uncoupler binding sites with an uncoupler capable of photoaffinity labeling. *J. Biol. Chem.* **249:**1356–1362
23. Haydon, D.A., Hladky, S.B. 1972. Ion transport across thin lipid membranes. A Critical discussion of mechanisms in selected systems. *Q. Rev. Biophys.* **5:**187–282
24. Helfferich, F. 1962. Ion Exchange. McGraw-Hill, New York
25. Hladky, S.B. 1974. The energy barriers to ion transport by nonactin across thin lipid bilayer membranes. *Biochim. Biophys. Acta* **352:**71–85
26. Holz, R., Finkelstein, A. 1970. The water and nonelectrolyte permeability induced in thin lipid membranes by the polyene antibiotics nystatin and amphotericin B. *J. Gen. Physiol.* **56:**125–145
27. Honig, B.H., Hubbell, W.L., Flewelling, R.F. 1986. Electrostatic interactions in membranes and proteins. *Annu. Rev. Biophys. Biophys. Chem.* **15:**163–193
28. Israelachvili, J.N. 1985. Intermolecular and Surface Forces. Academic, New York
29. Kasianowicz, J., Benz, R., McLaughlin, S. 1984. The kinetic mechanism by which CCCP (carbonyl cyanide *m*-chlorophenylhydrazone) transports protons across membranes. *J. Membrane Biol.* **82:**179–190
30. Katre, N.V., Wilson, D.F. 1977. Interaction of uncouplers with the mitochondrial membrane: A high-affinity binding site. *Arch. Biochem. Biophys.* **184:**578–585
31. Katre, N.V., Wilson, D.F. 1978. Interaction of uncouplers with the mitochondrial membrane: Identification of the high affinity binding site. *Arch. Biochem. Biophys.* **191:**647–656
32. Kell, D.B. 1979. On the functional proton current pathway of electron transport phosphorylation. An electrodic view. *Biochim. Biophys. Acta* **549:**55–99
33. Lauger, P., Neumcke, B. 1973. Theoretical analysis of ion conductance in lipid bilayer membranes. *In:* Membranes, a Series of Advances. G. Eisenman, editor. Vol. 2, pp. 1–59. Dekker, New York
34. LeBlanc, O.H., Jr. 1971. The effect of uncouplers of oxidative phosphorylation on lipid bilayer membranes. Carbonyl-cyanide *m*-chlorophenylhydrazone. *J. Membrane Biol.* **4:**227–251
35. Lowry, R.R., Tinsley, I.J. 1974. A simple sensitive method for lipid phosphorus. *Lipids* **9:**491–492
36. McLaughlin, S. 1977. Electrostatic potentials at membrane-solution interfaces. *Curr. Top. Membr. Transp.* **9:**71–144
37. McLaughlin, S.G.A., Dilger, J.P. 1980. Transport of protons across membranes by weak acids. *Physiol. Rev.* **60:**825–863
38. McLaughlin, S., Eisenberg, M. 1975. Antibiotics and membrane biology. *Annu. Rev. Biophys. Bioeng.* **4:**335–366
39. Mitchell, P. 1961. Coupling of phosphorylation to electron and hydrogen transfer by a chemiosmotic type of mechanism. *Nature (London)* **191:**144–148
40. Nachliel, E., Gutman, M. 1984. Kinetic analysis of proton transfer between reactants adsorbed to the same micelle. The effect of proximity on the rate constants. *Eur. J. Biochem.* **143:**83–88
41. Neumcke, B., Bamberg, E. 1975. The action of uncouplers on lipid bilayer membranes. *In:* Membranes. Vol. 3. G. Eisenman, editor. Dekker, New York
42. Neumcke, B., Lauger, P. 1969. Nonlinear electrical effects in lipid bilayer membranes: II. Integration of the generalized Nernst-Planck equations. *Biophys. J.* **9:**1160–1170
43. O'Shaughnessy, K., Hladky, S.B. 1983. Transient currents carried by the uncoupler, carbonyl cyanide *m*-chlorophenylhydrazone. *Biochim. Biophys. Acta* **724:**381–387
44. Parsegian, A. 1969. Energy of an ion crossing a low dielectric membrane. Solutions to four relevant electrostatics problems. *Nature (London)* **221:**844–846
45. Parsegian, A., Fuller, N., Rand, P. 1979. Measured work of deformation and repulsion of lecithin bilayers. *Proc. Natl. Acad. Sci. USA.* **76:**2750–2754
46. Prats, M., Teissie, J., Tocanne, J.-F. 1986. Lateral proton conduction at lipid water interfaces and its implications for the chemiosmotic-coupling hypothesis. *Nature (London)* **322:**756–758
47. Smejtek, P., Hsu, K., Perman, W.H. 1976. Electrical conductivity in lipid bilayer membranes induced by pentachlorophenol. *Biophys. J.* **16:**319–336
48. Szabo, G., Eisenman, G., McLaughlin, S.G.A., Krasne, S. 1972. Ionic probes of membrane structures. *Ann. N.Y. Acad. Sci.* **195:**273–290
49. Teissie, J., Prats, M., Soucaille, P., Tocanne, J.F. 1985. Evidence for conduction of protons along the interface between water and a polar lipid monolayer. *Proc. Natl. Acad. Sci. USA* **82:**3217–3221
50. Terada, H. 1981. The interaction of highly active uncouplers of oxidative phosphorylation with mitochondria. *Biochim. Biophys. Acta* **639:**225–242
51. Terada, H., Van Dam, K. 1975. On the stoichiometry between uncouplers of oxidative phosphorylation and respiratory chains: The catalytic action of SF-6847 (3,5-di-tert-butyl-4-hydroxybenzylidenemalonitrile). *Biochim. Biophys. Acta* **387:**507–518
52. Tsui, F.C., Ojcius, D.M., Hubbell, W.L. 1985. The intrinsic pK_a values for phosphatidylserine and phosphatidylethanolamine in phosphatidylcholine host bilayers. *Biophys. J.* **49:**459–468
53. Vetter, K.J. 1967. Electrochemical Kinetics: Theoretical Aspects. Academic, New York
54. Westerhoff, H.V., Chen, Y.-D. 1985. Stochastic free energy transduction: The role of independent, small coupling units. *Biochim. Biophys. Acta* **768:**257–292
55. Westerhoff, H.V., Melandri, B.A., Venturoli, G., Azzione, G.F., Kell, D.B. 1984. A minimal hypothesis for membrane-linked free-energy transduction: The role of independent, small coupling units. *Biochim. Biophys. Acta* **768:**257–292
56. Wilson, D.F., Ting, H.P., Koppleman, M.S. 1971. Mechanism of action of uncouplers of oxidative phosphorylation. *Biochemistry* **10:**2897–2902

Received 8 August 1986; revised 5 November 1986

Appendix I.

We first consider the steady-state current produced by a voltage of 100 mV when the pH = 8.3 and the [S-13] = 0.1 μM. From Eq. (5), and the value of $G(0, 0)$ in Fig. 6 and α in Fig. 9*b*, the steady-state current is $I(\infty) = 3 \times 10^{-4}$ A cm^{-2}. If the mechanism illustrated in Fig. 1*a* operates alone, the rate at which protons combine with adsorbed anions must be much greater than the current divided by the Faraday constant:

$$k_R[H^+]\{A^-\}'' \gg I(\infty)/F. \tag{A1}$$

(If the heterogeneous reaction at the interfaces limited the current, the steady-state current would saturate with an increase in voltage; it does not.) We know that $[H^+] = 5 \times 10^{-9}$ M and we have measured $\{A^-\} = (3 \times 10^{-2}$ cm) (10^{-7} M) by equilibrium techniques. When 100 mV is applied the steady-state value of $\{A^-\}'' \simeq 6 \times 10^{-12}$ moles cm^{-2}. We conclude that $k_R \gg 10^{11}$ M^{-1} sec^{-1} if the mechanism illustrated in Fig. 1*a* is to explain the steady-state current. The fastest protonation reactions that occur in the aqueous phase are slower than this value. Thus, even a model-independent calculation based on steady-state measurements leads us to conclude that the mechanism illustrated in Fig. 1*a* is not sufficient to account for the results. We can make a stronger, more precise, statement by considering the kinetic data.

A more detailed analysis of the voltage-clamp equations is required if we consider the possibility that the heterogeneous interfacial reactions in Fig. 1*a* are not at equilibrium [5]. When the reactions at the interfaces are not at equilibrium and $k_R < 10^{13}$ M^{-1} sec^{-1}, the magnitude of the relaxation, α, would be significantly larger than the value observed in our voltage-clamp experiments with S-13. Consider the case where the pH of the solution is 8.3 and the applied voltage is 25 mV. If we choose $k_A = 4 \times 10^3$ sec^{-1} $k_{HA} = 2 \times 10^4$ sec^{-1} and vary k_R from 10^{11} M^{-1} sec^{-1} to 10^{13} M^{-1} sec^{-1}, the model predicts α will vary from 182 to 6.2. If $k_R = 10^{14}$ M^{-1} sec^{-1}, $\alpha = 4.5$, a value in good agreement with the results of the kinetic experiments. The predicted value of the time constant, τ, also agrees with the results of the voltage-clamp experiments if $k_R = 10^{14}$ M^{-1} sec^{-1}. However, the predicted value of τ is less sensitive than α to the value of k_R. We conclude from the voltage-clamp data that $k_R > 10^{13}$ M^{-1} sec^{-1} if the mechanism illustrated in Fig. 1*a* is the main route by which protons cross the interface.

The charge pulse data lead us to similar conclusions. We solved numerically the charge pulse equations describing the model illustrated in Fig. 1*a* to examine what values of k_R are consistent with the experimental results [5]. The results of this analysis are given in Table A1. We fixed $k_A = 5 \times 10^3$ sec^{-1} and $N_o = 4$ pmol cm^{-2}, values consistent with the independent measurements reported above. We first assumed $k_R = 10^{11}$ M^{-1} sec^{-1}; this implies $k_D = 5 \times 10^3$ sec^{-1} if pK = 7.3. We then attempted to fit the experimental charge pulse results obtained from PC/chlorodecane membranes at pH = 8 by varying the value of k_{HA}. It is not possible to fit the experimental result for τ_2, even with values of k_{HA} as high as 10^7 sec^{-1} (Table A1). The rate limiting step is the protonation reaction: $k_R[H^+] = 10^3$ sec^{-1}. We then set $k_R = 10^{12}$ M^{-1} sec^{-1} (Table A1) and obtained a reasonable fit to the experimental data when $k_{HA} > 10^5$ sec^{-1}. However, if we set k_{HA} equal to the value obtained from the independent measurements, $k_{HA} = 3 \times 10^4$ sec^{-1}, we must set $k_R > 10^{13}$ M^{-1} sec^{-1} to obtain a good fit to the data. Thus, we must assume that the heterogeneous protonation reaction illustrated in Fig. 1*a* proceeds with a rate constant two orders of magnitude faster than a diffusion-controlled reaction in a bulk aqueous phase.

Table A1. Comparison between experimental data of charge pulse experiments and theoretical predictions of the model illustrated in Fig. 1*a*[a]

	τ_1 (μsec)	τ_2 (μsec)	a_2
Experimental results	16	110	0.25
Theoretical calculation for $k_R = 10^{11}$ M^{-1} sec^{-1}			
$k_{HA} = 10^4$ sec^{-1}	40	1600	0.21
$k_{HA} = 10^5$ sec^{-1}	20	1300	0.21
$k_{HA} = 10^7$ sec^{-1}	20	1300	0.21
Theoretical calculation for $k_R = 10^{12}$ M^{-1} sec^{-1}			
$k_{HA} = 10^4$ sec^{-1}	21	480	0.20
$k_{HA} = 10^5$ sec^{-1}	19	160	0.26
$k_{HA} = 10^7$ sec^{-1}	19	130	0.28
Theoretical calculation for $k_R = 10^{13}$ M^{-1} sec^{-1}			
$k_{HA} = 3 \times 10^4$ sec^{-1}	20	140	0.25

[a] The pH of the solution is 8.3 and the surface pK is assumed to be 7.3.

The analysis of the experimental charge pulse results obtained from PE/chlorodecane membranes in the presence of S-13 (Table 2) gave larger values for k_A (1.5×10^4 sec^{-1}) and k_{HA} (6.5×10^4 sec^{-1}) than we obtained with PC/chlorodecane membranes. To account for the experimental results with PE membranes, k_R must be about 10^{14} M^{-1} sec^{-1}, a value three orders of magnitude faster than the diffusion-controlled protonation rate constant observed in a bulk aqueous phase.

Thus, our analysis of the steady-state current, the voltage-clamp kinetic measurements and the charge pulse kinetic measurements leads us to similar conclusions: unless the diffusion coefficient of H^+ in the water adjacent to the membrane is anomalously high, the mechanism illustrated in Fig. 1*a* cannot be the main mechanism by which protons cross the interface.

Appendix II.

As illustrated in Fig. 1*c*, the rate at which protons are transferred from water directly to the adsorbed anions is:

$$k_3\{A^-\}''. \tag{B1}$$

If this is the main mechanism by which protons can cross the interface, this rate must be larger than the rate at which protons move from one aqueous phase to the other (the steady-state current, $I(\infty)$, divided by the Faraday constant). For pH 8.3, [S-

13] = 0.1 μM, V = 100 mV, we have for PC/chlorodecane membranes $I(\infty) = 3 \times 10^{-4}$ A cm^{-2} and $\{A^-\}'' = 6 \times 10^{-12}$ moles cm^{-2}, so we require:

$$k_3 > 5 \times 10^2 \text{ sec}^{-1}. \tag{B2}$$

For pH 7.3, the value of k_3 must be greater than 10^3 sec^{-1}. To calculate the value of k_3 we assume the water adjacent to the surface has the same properties as bulk water: the rate at which hydroxide ions combine with "normal" acids in bulk water is diffusion limited with a rate constant $\leq 10^{11}$ M^{-1} sec^{-1}. We assume $k_4 \leq 10^{11}$ M^{-1} sec^{-1} (Fig. 1*c*) for S-13. Our direct spectroscopic measurements demonstrate the surface pK of S-13 is about 7.3 or $K = 2 \times 10^7$ M^{-1}. If $K_W = [H^+][OH^-] = 10^{-14}$ M^2, the rate constant of the hydrolysis reaction is

$$k_3 = K_W k_4 K \leq 2 \times 10^4 \text{ sec}^{-1}. \tag{B3}$$

A realistic value for k_4 is probably 10^{10} M^{-1} sec^{-1}. This implies $k_3 = 2\ 10^3$ sec^{-1}. Thus, the hydrolysis reaction is barely fast enough to explain our experimental observation that the reactions illustrated in Fig. 1 are maintained approximately at equilibrium during our kinetic experiments for pH > 7.3. We conclude by noting that protons cross the membrane solution interface by mechanism 1*c* with a rate $k_3\{A^-\}''$ and by mechanism 1*a* with a rate $k_R\{A^-\}''[H^+]$. The ratio of these rates, R, is:

$$R = 10^{(-14 + \text{pH} + \text{pK})}. \tag{B4}$$

if $k_R = k_4$, which is approximately true for "normal" acids [12]. Eigen [11] discusses the relative importance of hydrolysis and protolysis reactions in detail. For bulk aqueous solutions, Eq. (B4) indicates that the hydrolysis reaction dominates when pH + pK > 14, or pH > 7 for S-13. Our experimental results are consistent with this prediction.